Available online at:
Al-Fiziya: Journal of Materials Science, Geophysics, Instrumentation and Theoretical Physics
Website: http://journal.uinjkt.ac.id/index.php/al-fiziya
Vol.7 No. II 2024, 1-13

SYNTHESIS AND CHARACTERIZATION OF ACTIVATED CARBON FROM MALAPARI PRESS CAKE, MALAPARI SHELL, AND CASSAVA PEEL

Sayida Ma'wa A'yuni [1*], Biaunik Niski Kumila[1], Arif Tjahjono[1]

[1]Department of Physics, Faculty of Sciences and Technology, State Islamic University Syarif Hidayatullah Jakarta, Indonesia.

[*]sayidamawa20@mhs.uinjkt.ac.id

Submitted: Ocktober; Revised: November; Approved: December; Available Online: December.

Abstract. Activated carbon is increasingly used in various applications, prompting researchers to innovate by utilizing biomass as a source for activated carbon. This study used biomass waste from malapari press cake, malapari shell, and cassava peel. The process involved carbonizing the samples at 500°C for 2 hours, chemical activation using a 65% (w/v%) KOH solution at a 1:4 ratio, stirring with a magnetic stirrer at 120°C and 300 rpm for 2 hours, followed by physical activation at 550°C for 1 hour, and BET & SEM-EDS testing. Based on the BET test results, the surface area of the samples increased overall between pre- and post-activation. The highest increase in surface area occurred in cassava peel, which increased from 7.916 m^2/g to 294.303 m^2/g. Meanwhile, the malapari press cake increased from 3.122 m^2/g to 11.445 m^2/g, and the malapari shell increased from 12.773 m^2/g to 105.320 m^2/g. SEM-EDS characterization revealed that cassava peel contained the highest carbon content at 67.02%, and after activation, each sample exhibited porous surfaces, uneven textures, and various pore shapes. ImageJ software analysis showed cassava peel had the smallest pore size at 123.209 nm, compared to malapari press cake at 234.721 nm and malapari shell at 217.419 nm. These results indicate that samples with larger surface areas tend to have smaller average pore sizes.

Keywords: *Activated carbon, biomass, BET, SEM-EDS.*
DOI : 10.15408/fiziya.v7i2.46256

INTRODUCTION

Activated carbon is a type of porous solid carbon that contains 85–95% carbon, with a vast surface area (from 300–3500 m^2/g), which can be achieved through carbon activation. Activated carbon is one of the most widely used adsorbents in adsorption processes. The production of activated carbon is carried out through carbonization and activation processes (high-temperature heating using steam, gases, and chemicals) that open the pores of the activated carbon to enhance adsorption [1], [2]. Activated carbon can be used in various applications, such as adsorbents (for iodine or phenol),

supercapacitors or battery electrodes, and catalysts [3], [4]. Due to the high demand for activated carbon, it is necessary to find effective and efficient methods for its production. One such approach is using raw materials that are abundant, easy to obtain, contain high amounts of carbon, and are renewable or unlimited. Researchers have thus conducted various innovations using biomass or plantation waste to produce activated carbon. Biomass materials with high carbon content, such as coconut shells, cassava peels, coconut fibers, palm kernel shells, wood, sugarcane bagasse, malapari press cake and shells, salak peels, and others, are potential sources of activated carbon.

The malapari plant is currently being promoted for biodiesel production from vegetable oil extracted from malapari fruits, with oil content ranging from 27–39% of the dry seed weight. This utilization does not compete with food production, as seen in India, where malapari is used as a vegetable oil source [5]. Approximately 50% of malapari oil is C18:1 (oleic acid), suitable for biodiesel production. Malapari biofuel has B100 quality (which can be used directly as diesel fuel) and meets the SNI standards [6], [7], [8]. Malapari was chosen as an alternative in efforts to develop biodiesel to prevent fossil fuel shortages in Indonesia [9], [10].

One hectare of malapari plants can yield about 9 tons of dry malapari seeds, with a sustainable production rate of over 50 years, with 1500–1700 seeds per kilogram [11]. Each tree can produce around 8–24 kg or 9–90 kg seed pods [6]. Previous studies have shown that 10 kg of malapari seeds produce only 1 liter of oil, leaving a significant amount of press cake residue [12]. The residual press cake is approximately two-thirds of the original seed weight, and malapari shells have not been optimally utilized [13]. It is necessary to study the use of malapari shells and press cake to produce valuable products that increase added value and reduce environmental pollution. Malapari press cake contains 26.6% crude protein, 5.6% crude fiber, 2.9% lignin, ether extract, and ash [8]. Malapari shells contain high levels of silica (SiO_2), making them quite complex, and also contain cellulose and lignin, which serve as carbon sources. Carbon-containing materials can be used as raw materials for producing activated carbon.

In a 2022 study by Ibrahim et al., malapari shells were characterized into activated carbon, showing optimal results under carbonization at 400°C with 2% H3PO4 activation, followed by activation at 750°C with steam for 60 minutes. This process produced a 54% yield, 63.42% bound carbon, iodine adsorption capacity of 648.62 mg/g, benzene adsorption capacity of 10.15%, methylene blue adsorption capacity of 93.89 mg/g, and a specific surface area of 348.11 m^2/g. This activated carbon still falls below the SNI standard [14]. A previous study by the same researchers in 2017 produced the best quality activated carbon at a carbonization stage of 450°C, activated with 2% H3PO4, followed by activation with steam at 750°C for 60 minutes, yielding a methylene blue adsorption capacity of 119.50 mg/g. The cleaning of activated carbon with 10% HCl increased the methylene blue adsorption capacity to 193 mg/g, meeting the SNI 06-3730-1995 standard, with a specific surface area of 715 m^2/g and pore surface area of 545.04 μm^2 [15].

Additionally, cassava peel has been widely used in activated carbon production. Cassava peel is a waste product from cassava tubers grown in various regions. It contains 59.31% carbon and chemical compounds (such as proteins, high levels of HCN (cyanide acid), and non-reducing cellulose) with functional groups like -OH, -NH2, -SH, and -CN. Thus, activated carbon can be used in cassava peel for metal ion-binding adsorbents [16]. According to Kurnia et al. (2023), cassava peel contains 43.6% cellulose, 10.38%

hemicellulose, 7.65% lignin, and other compounds that function as carbon sources [17]. In F.P. Perdani et al. (2021) study, the activated carbon from cassava peel characterization showed optimum KASP (cassava peel activated carbon) at a 30% H3PO4 concentration for 1 hour at 600°C. The morphology of KASP revealed a porous surface dominated by elements such as C (55.20%), O (28.86%), N (8.00%), P (6.22%), and Na (1.72%) [18]. A study by Apriliana Dwijayanti et al. (2020) characterized activated carbon from melinjo shells, showing the best quality activated carbon under chemical-physical activation at 550°C, with an iodine value of 695.53 mg/g and a surface area of 412.33 m^2/g [19].

METHODS

Chemicals and Instruments

The synthesis of activated carbon in this study was carried out at the Integrated Laboratory Center (PLT) of UIN Syarif Hidayatullah Jakarta, and sample testing and characterization were conducted at the ILRC UI Lab (BET testing) and SEM ITB Lab (SEM-EDS characterization). Biomass materials such as press cake malapari, malapari shells, and cassava peel were used in this study. Carbonization of all samples was performed at 500°C for 2 hours. Chemical activation was carried out using a 65% (w/v) KOH solution with a 1:4 ratio, and physical activation was performed in a furnace for 1 hour at 550°C. Distilled water and 2 M HCl were used to wash the activated carbon samples.

Synthesis of Activated Carbon

Activated Carbon of Press Cake and Malapari Shells

The malapari press cake and shells used in this study were sourced from Parungpanjang, Bogor Regency (obtained from Ciheuleut). The malapari shells were cleaned first and washed with distilled water until thoroughly cleaned. In contrast, the press cake was only cleaned to remove surface impurities without washing with distilled water due to its fragile nature. The material was then sun-dried and dried in an oven to reduce its moisture content at 130°C for 1 hour. Next, the press cake and malapari shells were carbonized in a furnace at 500°C for 2 hours. The carbonized samples were cleaned of any formed ash, ground using a mortar, and sieved through a 200-mesh sieve. The sieved press cake and malapari shell samples were washed with distilled water until neutral pH (pH = 7) to remove any remaining ash. The samples were then dehydrated in an oven at 125°C for 50 minutes (for press cake) and at 130°C for 45 minutes (for malapari shells). Each carbonized sample (25 grams) was subjected to chemical activation using a 65% (w/v) KOH solution at a 1:4 ratio for 24 hours. After chemical activation, the samples were stirred using a magnetic stirrer for 2 hours at 120°C with a speed of 300 rpm. After stirring, the samples were filtered using filter paper and dehydrated in an oven at 130°C for 50 minutes (for press cake carbon) and at 130°C for 45 minutes (for malapari shell carbon). The next step was physically activating the samples with chemical activation, using a furnace at 550°C for 1 hour. After physical activation, the carbon samples were washed with distilled water and 2 M HCl until neutral pH (pH = 7) and then dehydrated in an oven.

Table 1 Variations and sample codes of malapari press cake and shells.

No.	Sample Code	Variation of Sample
1.	KAM	Malapari press cake before activation
2.	KAM2	Malapari press cake after chemical and physical activation
3.	KCM	Malapari shell before activation
4.	KCM2	Malapari shell after chemical and physical activation

Activated Carbon of Cassava Peels

The cassava peels used in this study were obtained from Teluk Pinang Village, Ciawi. The cassava peels were cleaned, then cut into pieces approximately 2×3 cm, and washed with distilled water until thoroughly cleaned. After cleaning, the cassava peels were sun-dried and further dried in an oven to reduce their moisture content to 145°C for 1 hour and 30 minutes. The process for producing activated carbon from cassava peels was the same as that used for press cake and malapari shells (with the only difference being the temperature and duration of sample dehydration), including carbonization at 500°C for 2 hours, grinding and sieving through a 200 mesh sieve, chemical activation using a 65% (w/v) KOH solution at a 1:4 ratio for 24 hours, stirring the sample with a magnetic stirrer for 2 hours at 120°C with a speed of 300 rpm, and physical activation at 550°C for 1 hour.

Table 2 Variations and sample codes of cassava peels.

No.	Sample Code	Variation of Sample
1.	KKS	Cassava peel before activation
2.	KKS2	Cassava peel after chemical and physical activation

Sample Characterization

The tests conducted in this study include BET (Brunauer, Emmett, and Teller) analysis to determine the surface area and isotherm graph of the activated carbon samples before and after activation. The BET test in this study was carried out using a Quantachrome QuadraWin ©2000-16 device with a degassing temperature of 150°C for 4 hours, and nitrogen (N_2) was used as the adsorbate at a temperature of 77.350 K. The characterization includes SEM-EDS to determine the activated carbon's elemental content and surface morphology from press cake, malapari shells, and cassava peels. The SEM-EDS characterization was carried out using a JOEL JSM-6510 LA instrument. EDS testing was performed to determine the chemical composition of a sample at a voltage of 15 kV and magnification of 1500X. For SEM morphological characterization, a voltage of 10 kV was used, with magnifications of 5000X and 15000X. Subsequently, analysis was performed using ImageJ and OriginLab software.

RESULTS AND DISCUSSION

Results of Changes in Activated Carbon Mass

The synthesis of activated carbon generally involves several stages, such as carbonization, activation, and testing. During this synthesis process, changes in the mass of each sample occur, particularly during the high-temperature carbonization stage, which takes a considerable amount of time, and the characteristics of the material used also influence the results. Carbonization is the process of carbon from the decomposition

of organic materials, with oxygen and hydrogen removed from the carbon, resulting in carbon with a specific structure (usually imperfect). Carbon formation occurs between 400–600ºC [11], [12]. Table 3 below shows the variation in mass changes in samples of malapari press cake, malapari shells, and cassava peels before and after carbonization.

Table 3 Variation in mass changes in samples of malapari press cake, malapari shells, and cassava peels before and after carbonization.

Types of Carbon	Before Carbonization (gram)	After Carbonization (gram)	Reduction (%)
Malapari Press Cake	146.2	43.4	70.315
Malapari Shells	96.5	41.6	56.891
Cassava Peels	88.8	18.1	79.617

Each sample experienced a significant mass reduction of more than 50% before and after carbonization; cassava peels showed the highest mass reduction of 79.617%, resulting in only 18.1 grams of carbon in Table 3. When the carbonization temperature is too high, the pore structure that forms may be damaged, reducing the surface area and adsorption properties and increasing the formation of ash from volatile substances, which also depends on the characteristics of the material used [19]. Subsequently, chemical and physical activation processes were carried out to activate the carbon into activated carbon. Table 4 shows the mass of the samples before and after chemical and physical activation.

Table 4 Variation in mass changes in samples of malapari press cake, malapari shells, and cassava peels before and after chemical and physical activation.

Types of Carbon	Before Chemical and Physical Activation (m^2/g)	After Chemical and Physical Activation (m^2/g)	Reduction (%)
Malapari Press Cake	25	23.7	5.2
Malapari Shells	25	20.9	16.4
Cassava Peels	15	11.8	21.3

It can be observed in Table 4 that the mass of each carbon sample before and after activation experienced a reduction, which may be caused by several factors, such as during the high-temperature heating process (activation and/or dehydration), where mass decreases due to the rapid evaporation of volatile substances (organic compounds, water, volatiles) that transform into ash. The remaining sample or spillage may also contribute to the mass loss [2], [20], [21]. After the synthesis process, the activated carbon samples were tested and characterized using BET (Quantachrome QuadraWin ©2000-16) and SEM-EDS (JOEL JSM-6510 LA).

BET Surface Area and Isotherm Graph Results

The BET test determined the samples' surface area and isotherm graph. Before being tested and analyzed by BET, the samples were first degassed. Degassing was performed before testing to remove any impurities or residues from the samples, ensuring they were cleaner for the subsequent analysis stage [8]. Table 5 below presents the results of the BET test, showing the surface area of the activated carbon samples before and after chemical and physical activation.

Table 5. Results of the BET test show the surface area before and after chemical and physical activation.

Types of Carbon	Before Chemical and Physical Activation (m^2/g)	After Chemical and Physical Activation (m^2/g)	Increase (%)
Malapari Press Cake	3.122	11.445	366%
Malapari Shells	12.773	105.320	824.6%
Cassava Peels	7.916	294.303	3717.8%

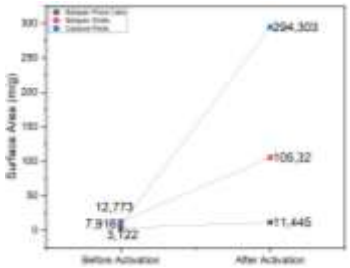

Figure. 1 BET surface area graph of 3 materials before and after chemical and physical activation.

Based on the results in Table 3 and Figure 1, the overall surface area of the samples, both before and after activation, showed a significant increase because of the activation process. The largest surface area was obtained from the activated carbon sample of cassava peels after activation, with a value of 294.303 m^2/g, approaching the minimum standard of 300 m^2/g [22]. This result indicates that the activation process was more successful and optimal for this sample than the other two variations in opening and expanding the activated carbon pores under the same parameters.

The large surface area of the cassava peel-activated carbon sample suggests that it contains a higher amount of cellulose and hemicellulose. Kurnia et al. (2023) explain that cassava peels contain 43.6% cellulose, 10.38% hemicellulose, and 7.65% lignin. These components contribute to forming an optimal pore structure, and their reactivity increases during the activation process. The higher the cellulose, hemicellulose, and lignin content in biomass, the better the quality of the activated carbon produced [23]. Cellulose aids in the formation of a more orderly, homogeneous, and stable pore structure, thereby increasing its surface area [24]. A higher hemicellulose content improves reactivity and effectiveness during chemical activation [25]. The right amount of lignin can enhance the surface area of activated carbon and provide structural strength. However, excessive lignin content, particularly with a high mineral content, can form ash during high-temperature heating, covering the pores and reducing the effective surface area [24].

On the other hand, the activated carbon samples from press cake and malapari shells showed smaller surface areas, indicating lower cellulose and hemicellulose content, and therefore fewer and less optimal pores were formed [26]. In the studies by Ibrahim et al. (2017 and 2022), the specific surface area of activated malapari shell carbon was significantly larger, 715 m^2/g and 348.11 m^2/g, respectively, compared to the surface area of malapari shell carbon in this study, which was only 105.32 m^2/g [14], [15]. The small surface area can be attributed to several factors, such as less effective activation (due to activator concentration and type of activator used), inefficient synthesis processes (such

as excessively high and prolonged carbonization or activation temperatures, leading to excessive ash formation that hinders pore development), and differences in the carbonization and activation equipment used. For instance, a pyrolysis furnace with steam assistance was used in previous studies, while this study employed a standard furnace [27], [28].

In addition to surface area data, adsorption isotherm data were also obtained from the tested samples, which represent the relative pressure (P/Po) against the volume of adsorbate adsorbed on the adsorbent surface (sample) under Standard Temperature and Pressure (STP) conditions [29]. Below is the isotherm graph for the six samples and the table of average adsorption volume.

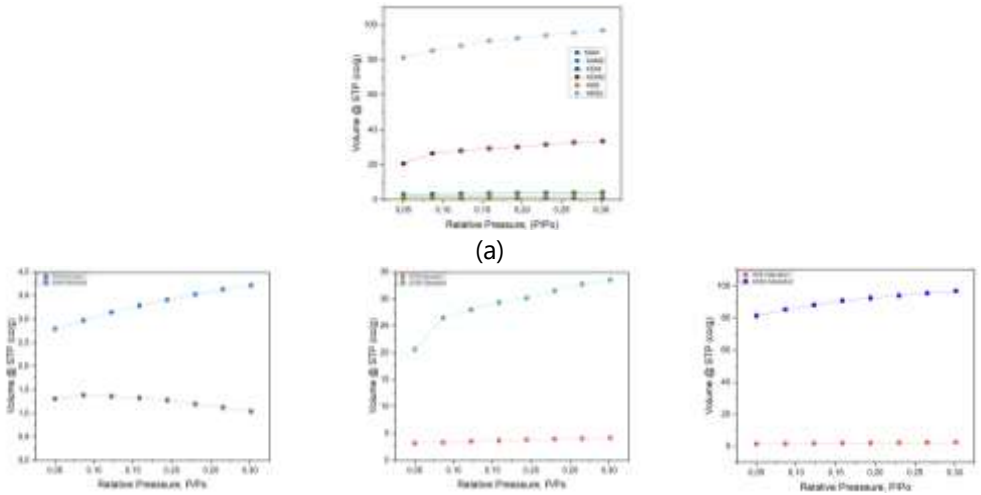

(a) (b) (c) (d)

Figure. 2 Isotherm graph of (a) all samples, (b) KAM and KAM2, (c) KCM and KCM2, and KKS and KKS2.

Table 6 Average Adsorption Volume of BET Isotherm Test at 8 Points.

Sample Carbon Code	Average Adsorption Volume of BET Isotherm Test at 8 Points (cc/g)	Highest Adsorption Volume of BET Isotherm Test at 8 Points (cc/g)
KAM	1.2484	1.3804
KAM2	3.306713	3.7157
KCM	3.689013	4.1557
KCM2	29.0308	33.4929
KKS	1.961138	2.4846
KKS2	90.41511	96.7376

In the isotherm volume graph, relative pressure indicates the partial pressure of the adsorbate (N_2) compared to the vapor pressure of N_2 at 77.35 K. Figure 2 (a) shows that the sample with the highest adsorption volume is the activated carbon of cassava peels after activation, while the lowest is from the press cake carbon sample before activation. Figure 2 (b) presents the data for the KAM sample, where the highest adsorption volume is 1.3804 cc/g. The adsorption volume increases at low pressure but then decreases at the third point (from 1.3804 cc/g to 1.3567 cc/g) as the relative pressure increases. This result indicates the occurrence of capillary condensation in the larger pores or the packing effect [30]. The increase and decrease in adsorption volume suggest that the pores in the KAM sample are beginning to be fully occupied, and there is no more room

for N_2 molecules at higher pressure. Once the maximum is reached, the adsorption volume starts to decrease. Meanwhile, in the KAM2 isotherm graph, it is shown that as the P/Po value increases, the adsorbed volume also increases, meaning more N_2 gas is being adsorbed, with the highest adsorption volume reaching 3.7157 cc/g [24], [29]. In Figure 2 (c), the adsorption isotherm graph for the KCM sample shows the highest adsorption volume of 4.1557 cc/g, with a relatively small increase and remaining nearly constant. In comparison, KCM2 reaches 33.4929 cc/g, with a higher increase that tends to be steady. In Figure 2 (d), the adsorption isotherm graph for the KKS sample shows the highest adsorption volume of 2.4846 cc/g, which increases relatively slowly. KKS2 reaches 96.7376 cc/g, with a higher increase and a nearly constant value. The results of the KKS2 adsorption volume are the highest, indicating better adsorption performance than the other samples. This is correlated with the highest surface area of the KKS2 sample, which is 294.709 m^2/g, suggesting that the larger the activated carbon's surface area, the more active sites, or pores on the surface, can bind N_2 gas, leading to a higher adsorption volume [31].

SEM-EDS (Element Content and Morphology) Results

The characterization in this study used SEM-EDS to determine the activated carbon's elemental content and surface morphology. The following table shows the elemental content from the EDS analysis results.

Table 7 Elemental Content of KAM2, KCM2, and KKS2 Samples.

Sample Name	Elemental Content (mass%)												
	C	N	O	Na	Mg	Cl	K	Ca	Br	Rb	Cu	Al	P
KAM2	62.61	22.53	1.60	-	0.82	-	8.00	2.02	-	-	-	0.78	1.64
KCM2	66.12	24.62	1.57	0.14	0.69	0.27	3.37	1.45	1.61	0.17	-	-	-
KKS2	67.02	26.94	0.72	0.13	0.95	0.39	1.39	2.12	-	-	0.33	-	-

Based on the results of the EDS analysis, all three samples have almost identical carbon content. EDS analysis found that the KKS2 sample has the highest carbon content at 67.02%. With cellulose content of 43.6%, hemicellulose at 10.38%, and lignin at 7.65%, which were relatively high in cassava peel, Kurnia et al. (2023) found that higher activated carbon yield occurs due to cellulose, hemicellulose, and lignin being carbon sources, with the highest carbon content being detected [32].

According to Kumar (2007), malapari press cake contains 5.6% dry-weight hemicellulose and 2.9% dry-weight lignin, indicating that with such content, carbon yields above 60% can be obtained, which is not much different from the other samples. However, it has the lowest carbon percentage [8]. The carbon percentage in KAM2 is relatively high. However, its surface area of only 11.445 m^2/g may be attributed to several factors, such as contamination by impurities that reduce surface area and block the pores of the activated carbon, hindering its adsorption capacity. Additionally, the activation method may have been inappropriate or suboptimal, thus not effective in increasing surface area, and the low activation temperature might not have been sufficient to clean the pores and improve their structure [27], [28]. For the malapari shell sample (KCM2), no literature regarding the cellulose and lignin content is available. However, it can be inferred that the cellulose, hemicellulose, and lignin content in the malapari shell is

relatively high. Therefore, during the carbonization and activation process at these temperatures, a relatively large amount of carbon is expected to be produced [32]. It can also be observed in Table 7 that the KKS2 sample detected a trace amount of copper (Cu) at 0.33%, which is attributed to non-technical errors during the synthesis process. Although Cu was detected, this indicates that the Cu element entered during the middle or final stages of the synthesis process, so it did not significantly interfere with the activation process, resulting in the largest surface area. Meanwhile, the KAM2 sample detected aluminum (Al) at 0.78% (a higher percentage). The presence of Al suggests that this element entered the sample during the synthesis process and caused contamination during the initial activation stage, which obstructed or hindered the pore-opening process, thus interfering with the activation process. This result could be one of the reasons the KAM2 sample has the smallest surface area [28].

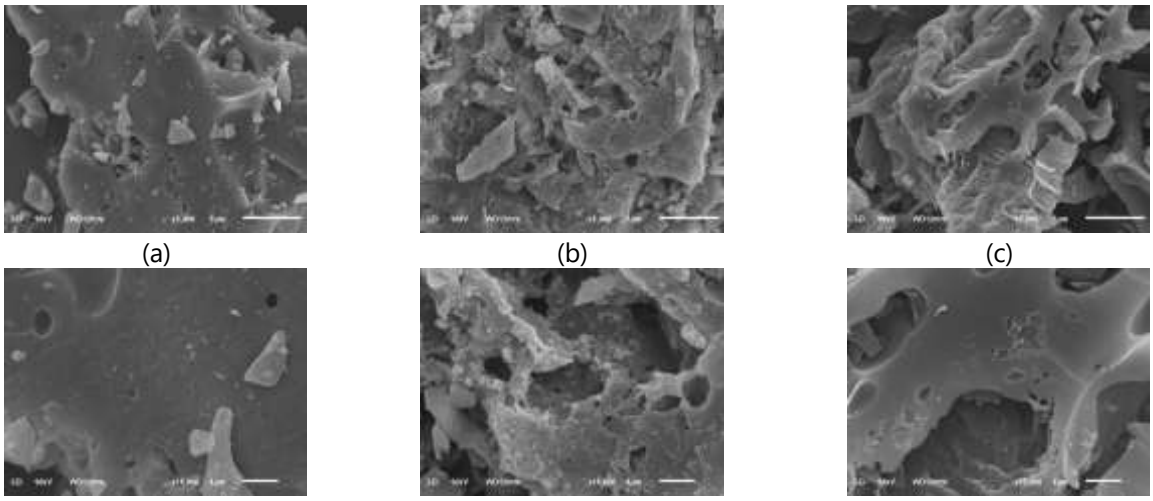

Figure. 3 Surface Morphology of samples at 5000X (a) KAM2, (b) KCM2, (c) KKS2, and at 15000X (d) KAM2, (e) KCM2, (f) KKS2.

Based on Figure 3, the surface morphology of the three activated samples shows the formation of pores, indicated by the presence of holes/cavities on the surface. However, a honeycomb-like porous structure has not yet formed. This suggests that the activation process may not have been optimal in opening new pores and creating an ideal pore structure, as reported in previous studies [33], [34], [35], [36]. Within the pores of each sample, there are smaller and larger particles, such as fragments, trapped or adhering to the pore walls and surface, indicating residues from the raw material or activation process. The KAM2 sample (Fig. 3 (a) & (d)), with the smallest surface area, has fewer and larger pores compared to KKS2 and KCM2, indicating that fewer pores lead to a smaller surface area, with fewer active sites for adsorption [37]. The surface texture is uneven, with various pore shapes and higher distances between pores (lower porosity) than in the other samples. The KCM2 sample has a more complex pore morphology than KAM2 (consistent with its larger surface area), with uneven pore walls, more pores of varying sizes, and a rougher surface texture. The KKS2 sample (Fig. 3 (c) & (f)) has the most complex pore structure, with thin and uneven surfaces and varying pore sizes (ranging from minor to larger pores). At a magnification of 15000X, the pores of the KKS2

sample are mostly smaller. Based on the largest surface area and numerous smaller pores, the porosity of the KKS2 sample is higher than that of the KAM2 and KCM2 samples [38].

The estimation of pore size from the SEM surface morphology was carried out using ImageJ software. The number of pores counted for each sample depends on the visible pores in the SEM images at 15000X magnification (where the pore shapes are more precise at higher resolution). The estimated average pore size was calculated using the following equation for the samples:

$$\bar{D} = \frac{\mathrm{D1} + \mathrm{D2} + \mathrm{D3} + \mathrm{D4} + \mathrm{D5} + \mathrm{D6}}{6} \quad (1)$$

where $\bar{D}$ represents the average pore size; D1, D3, D4 are the pore sizes in the horizontal direction; D2, D5, D6 are the pore sizes in the vertical direction. The following table shows the average pore size of the KAM2, KCM2, and KKS2 samples.

Table 8 Average Pore Size of KAM2, KCM2, and KKS2 Samples at 15000X Magnification.

Sample of Activated Carbon	Average Pore Size* (nm)	Average Pore Size† (nm)
KAM2	234.721	290.095
KCM2	217.419	278.257
KKS2	123.209	151.881

*Pore size using six lines from each visible pore.
†Pore size using the longest single line from each visible pore.

Average pore size results from ImageJ software indicate that the KKS2 sample has the smallest average pore size, 123.209 nm. This smaller pore size is directly related to the surface area of the activated carbon; the smaller the pore size, the more pores can form on the sample's surface, increasing its surface area and making it more suitable for adsorbing small molecules and vice versa [37]. In the KAM2 sample, the pores are visibly larger and fewer at 15000X magnification, with an average pore size of 234.721 nm, corresponding to the smallest surface area of activated carbon from malapari waste, which is only 11.445 m^2/g. Below is the histogram distribution of pore sizes for KAM2, KCM2, and KKS2 samples.

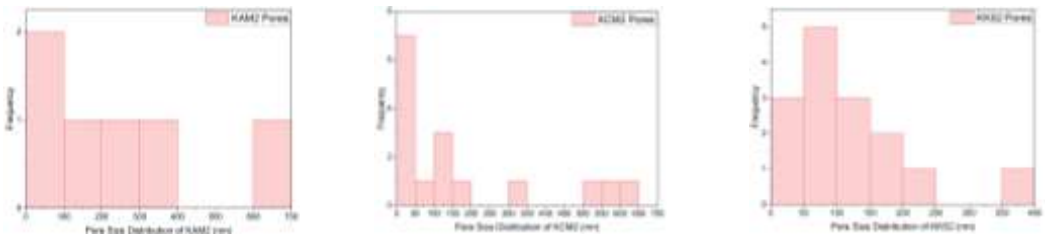

(a) (b) (c)

Figure. 4 (a) Pore Size Distribution of KAM2 Sample, (b) Pore Size Distribution of KCM2 Sample, and (c) Pore Size Distribution of KKS2 Sample.

Based on Figure 4, the pore size distribution for each sample varies (from < 50 nm to > 50 nm); it can be concluded that each sample contains mesoporous and macroporous structures (dominated by macropores/large pores). The KAM2 sample, with fewer and larger pores, indicates that contamination by foreign substances (e.g., Al metal) significantly affects the pore formation in malapari press cake, leading to suboptimal

pore development [39]. Based on the average pore size results, all three samples fall into the macroporous structure category (> 50 nm) and can be applied in areas such as water and waste treatment, chemical purification, air purification, energy storage, and more [[40], [41].

CONCLUSION

Biomass can be utilized as an activated carbon material for various applications. In this study, biomass used included malapari press cake, malapari shell, and cassava peel. The process steps included carbonization at 500°C for 2 hours, chemical activation using a 65% (w/v) KOH solution at a 1:4 ratio, stirring with a magnetic stirrer at 120°C, 300 rpm for 2 hours, and physical activation at 550°C for 1 hour. The surface area of all samples increased, with the highest increase seen in cassava peel, from 7.916 m^2/g to 294.303 m^2/g. Meanwhile, malapari waste increased from 3.122 m^2/g to 11.445 m^2/g, and malapari shell increased from 12.773 m^2/g to 105.320 m^2/g. SEM-EDS characterization showed cassava peel contains the highest carbon content at 67.02%, and all samples have pore structures with varying shapes and uneven surfaces. ImageJ software analysis showed cassava peel had the smallest average pore size of 123.209 nm, compared to malapari press cake at 234.721 nm and malapari shell at 217.419 nm. These results indicate that samples with larger surface areas tend to have smaller average pore sizes. Therefore, further research using different variables is needed to achieve better-activated carbon results, especially for the malapari press cake and shells biomass.

ACKNOWLEDGMENTS

We sincerely thank Dr. Aam Aminah, S. Hut., M.Si. for kindly providing the malapari press cake and shell materials for this research. Thanks to the Material Physics Laboratory and the Chemistry Laboratory at the Integrated Laboratory Center (PLT) UIN Jakarta, the ILRC Laboratory at UI, and the SEM Laboratory at FMIPA ITB for their support in sample preparation and testing during this study.

REFERENCES

[1] L. F. Ramadhani, I. M. Nurjannah, R. Yulistiani, and E. A. Saputro, "Review: teknologi aktivasi fisika pada pembuatan karbon aktif dari limbah tempurung kelapa," 2020.

[2] A. Monarita, N. Sylvia, N. ZA, I. Ibrahim, and R. Dewi, "Optimasi Proses Pembuatan Karbon Aktif Dari Kulit Singkong Menggunakan Aktivator ZnCl2," *Teknologi Kimia Unimal*, vol. 1, pp. 66–75, 2022.

[3] L. M. Yuningsih, D. Mulyadi, and A. J. Kurnia, "Pengaruh Aktivasi Arang Aktif dari Tongkol Jagung dan Tempurung Kelapa Terhadap Luas Permukaan dan Daya Jerap Iodin," *Jurnal Kimia VALENSI*, vol. 2, no. 1, pp. 30–34, May 2016, doi: 10.15408/jkv.v2i1.3091.

[4] A. Prayogatama and T. Kurniawan, "Modifikasi Karbon Aktif dengan Aktivasi Kimia dan Fisika Menjadi Elektroda Superkapasitor," *Jurnal Sains dan Teknologi*, vol. 11, pp. 47–58, 2022, doi: 10.23887/jst-undiksha.v11i1.

[5] D. Alimah, "Budidaya dan Potensi Malapari (Pongamia pinnata L. Piere) Sebagai Tanaman Penghasil Bahan Bakar Nabati," *Galam*, vol. 5, no. 1, pp. 35–49, 2011, [Online]. Available: https://www.researchgate.net/publication/344538551

[6] V. Lakshmikanthan, *Tree Borne Oilseeds*. Mumbai, India: Directorate of Nonedible Oils & Soap Industry, Khadi and Village Industries Commission, 1978.
[7] Badan Standarisasi Nasional (BSN), *SNI 04-7182-2006 Biodiesel*. Jakarta: Badan Standarisasi Nasional, 2006.
[8] S. Kumar, J. Ramadhani, A. K. Singh, and K. S. Varaprasad, "Germination and Seed Storage Behaviour in Pongamia pinnata L.," *Curr Sci*, vol. 93, no. 7, 2007.
[9] KNRT, *Buku Putih: Penelitian, Pengembangan dan Penerapan Ilmu Pengetahuan dan Teknologi Bidang Sumber Energi Baru dan Terbarukan untuk Mendukung Keamanan Ketersediaan Energi Tahun 2025*. Jakarta: Kementerian Negara Riset dan Teknologi (KNRT), 2006.
[10] Jayusman, "Penetapan Strategi Pemuliaan untuk Mendukung Pengembangan Malapari (Pongamia pinnata L.) sebagai Penghasil Biofuel," in *Proceeding Biology Education Conference*, 2018, pp. 737–742.
[11] Mardjono, "Mengenal ki pahang (Pongamia pinnata) sebagai bahan bakar alternatif harapan masa depan," *Warta Penelitian dan Pengembangan Tanaman Industri 14*, pp. 14–34, 2008.
[12] A. Aminah, Z. Siregar, and D. A. Suryani, "Kandungan Minyak Malapari (Pongamia Pinnata (L.) Pierre) Dari Pulau Jawa Sebagai Sumber Bahan Baku Biodiesel," *Penelitian Hasil Hutan* , vol. 35, no. 4, pp. 255–262, 2017, doi: 10.20886/jphh.2017.35.3.255-262.
[13] B. Vinay and T. Kanya, "Effect of detoxification on the functional and nutritional quality of proteins of karanja seed meal," *Food Chem*, vol. 106, pp. 77–84, 2008.
[14] I. Ibrahim, D. Hendra, N. Adi Saputra, and E. Rohaeti, "Karakteristik Karbon Aktif dari Kulit Buah Malapari (Pongamia pinnata L. Pierre)," *Jurnal Penelitian Hasil Hutan*, vol. 40, no. 1, pp. 1–6, Apr. 2022, doi: 10.20886/jphh.2022.40.1.1-6.
[15] Ibrahim, E. Rohaeti, and D. Hendra, "Synthesis Activated Charcoal of Malapari (Pongamia pinnata) Fruit peel," *Advances in Health Science Research*, vol. 6, 2017.
[16] A. R. Permatasari *et al.*, "Karakterisasi Karbon Aktif Kulit Singkong (Manihot Utilissima) Dengan Variasi Jenis Aktivator," 2014.
[17] Kurnia *et al.*, "Cassava Peel Extract as Raw Materials for Making Paper : Utilization of Waste as Environmental Conservation," *International Journal of Hydrological and Environmental for Sustainability*, vol. 1, no. 3, pp. 160–168, 2023.
[18] F. Puteri Perdani, C. Alep Riyanto, and Y. Martono, "Karakterisasi Karbon Aktif Kulit Singkong (Manihot esculenta Crantz) Berdasarkan Variasi Konsentrasi H3PO4 dan Lama Waktu Aktivasi," *Ind. J. Chem. Anal*, vol. 04, no. 02, pp. 72–81, 2021, doi: 10.20885/ijca.vol4.iss2.art4.
[19] A. Dwijayanti, S. Kartika, Slamet, and Yuliusman, "Characterization of Activated Carbon from Melinjo (Gnetum gnemon) Shells with Chemical-Physical Activation," *Advances in Social Science, Education and Humanities Research*, vol. 410, pp. 49–51, Mar. 2020, doi: 10.2991/assehr.k.200303.014.
[20] A. Dwijayanti, S. Kartika, and Yuliusman, "The effect of carbonization temperature and activator to the characteristics of melinjo shell (Gnetum genom) activated carbon," in *AIP Conference Proceedings*, American Institute of Physics Inc., Nov. 2019. doi: 10.1063/1.5134621.
[21] H. Marsh and F. Rodríguez-Reinoso, "CHAPTER 9 - Production and Reference Material," *Activated Carbon*, pp. 454–508, 2006.
[22] S. Wardani *et al.*, "Potensi Karbon Aktif Kulit Pisang Kepok (Musa Acuminate L) Dalam Menyerap Gas CO Dan SO 2 Pada Emisi Kenderaan Bermotor," *Serambi Engineering*, vol. III, no. 1, 2018.
[23] Y. Takeuchi, *An Introduction to Chemistry*. Tokyo: Iwanami Publishing Company, 2006.
[24] Neneng Purnamawati, "UJI KUALITAS SINTESIS KARBON AKTIF DARI PELEPAH AREN TERAKTIVASI ASAM FOSFAT," *Journal of Research and Education Chemistry*, vol. 5, no. 2, p. 120, Dec. 2023, doi: 10.25299/jrec.2023.vol5(2).15225.

[25] M. Rizki Bina, Syaruddin, L. O. Sahara, and M. Sayuti, "KANDUNGAN SELULOSA, HEMISELULOSA DAN LIGNIN DALAM SILASE RANSUM KOMPLIT DENGAN TARAF JERAMI SORGUM (Sorghum bicolor (L.) Moench) YANG BERBEDA," *Gorontalo Journal of Equatorial Animals*, vol. 2, no. 1, pp. 44–53, 2023.

[26] H. Nurdiansah and D. Susanti, "Pengaruh Variasi Temperatur Karbonisasi dan Temperatur Aktivasi Fisika dari Elektroda Karbon Aktif Tempurung Kelapa dan Tempurung Kluwak Terhadap Nilai Kapasitansi Electric Double Layer Capacitor (EDLC)," *TEKNIK POMITS*, vol. 2, no. 1, 2013.

[27] A. Cahyadi and I. Prasetyo, "PENGARUH LUAS PERMUKAAN DAN LEBAR PORI KARBON AKTIF PADA SISTEM ADSORBED NATURAL GAS (ANG)," Universitas Gajah Mada, Yogyakarta, 2013.

[28] M. Sudibandriyo, "KARAKTERISTIK LUAS PERMUKAAN KARBON AKTIF DARI AMPAS TEBU DENGAN AKTIVASI KIMIA," 2011.

[29] A. Ladavos, A. Katsoulidis, A. Iosifidis, K. Triantafyllidis, and et. al, "BET equation, inflection point of N2 adsorption isotherm, and estimation of specific surface area of porous solids," *Microporous and Mesoporious Materials*, vol. 151, pp. 126–133, 2012.

[30] A. M. Elewa, A. A. Amer, M. F. Attallah, and et. al, "Chemically Activated Carbon Based on Biomass for Adsorption of Fe(III) and Mn(II) Ions from Aqueous Solution," *Materials*, vol. 16, no. 1251, pp. 1–21, 2023.

[31] N. P. Cheremisinoff, *Handbook of Water and Wastewater Treatment Technologies*. 2002.

[32] P. González-García, "Activated carbon from lignocellulosics precursors: A review of the synthesis methods, characterization techniques and applications," *Renewable and Sustainable Energy Reviews*, pp. 1393–2424, 2018.

[33] T. E. Amakoromo, O. E. Abumere, J. A. Amusan, V. Anye, and A. Bello, "Porous carbon from Manihot Esculenta (cassava) peels waste for charge storage applications," *Current Research in Green and Sustainable Chemistry*, vol. 4, Jan. 2021, doi: 10.1016/j.crgsc.2021.100098.

[34] Rinawati R, Kiswandono AK, Widiarto S, Kasih YO, and Hadi S, "Study on Activated Carbon derived from Cassava Peels as Magnetic Solid of Dispersive Solid Phase Extraction Technique for Determination of Tetracycline," *Res J Chem Environ*, vol. 27, no. 3, pp. 1–8, 2023.

[35] W. Astuti, M. Hidayah, L. Fitriana, M. A. Mahardhika, and E. F. Irchamsyah, "Preparation of activated carbon from cassava peel by microwave-induced H3PO4 activation for naphthol blue-black removal," in *AIP Conference Proceedings*, American Institute of Physics Inc., Jun. 2020. doi: 10.1063/5.0001464.

[36] R. Kayiwa, H. Kasedde, M. Lubwama, and J. B. Kirabira, "Active Pharmaceutical Ingredients Sequestrated from Water Using Novel Mesoporous Activated Carbon Optimally Prepared from Cassava Peels," *Water (Switzerland)*, vol. 14, no. 21, Nov. 2022, doi: 10.3390/w14213371.

[37] R. Joni, S. Syukri, and H. Aziz, "Study of activated carbon characteristic from ketaping fruit shell (Terminalia Catappa) as supercapasitors electrode," *Journal of Aceh Physics Society*, vol. 10, no. 1, pp. 1–6, Jan. 2020, doi: 10.24815/jacps.v10i1.17755.

[38] M. A. Mardiah, A. Awitdrus, R. Farma, and E. Taer, "Characterization of Physical Properties for Activated Carbon from Garlic Skin," *Journal of Aceh Physics Society*, vol. 10, no. 4, pp. 102–106, Oct. 2021, doi: 10.24815/jacps.v10i4.19571.

[39] A. Primastiyaningayu, E. I. Rismala, and N. W. Triana, "Sintesa dan Karakteristik Karbon Aktif dari Batang Pisang Kepok (Musa acuminata) Sebagai Adsorben pada Penjernihan Minyak Goreng Bekas," *Jurnal Ilmiah Teknik Kimia*, vol. 8, no. 2, pp. 83–90, Aug. 2024, doi: 10.32493/jitk.v8i2.40221.

[40] Sharma and et al, "Health Hazards of Hexavalent Chromium and Its Removal Using Activated Carbon," *J Environ Manage*, vol. 13, no. 3, pp. 4923–4938, 2022, [Online]. Available: https://doi.org/10.1080/21655979.2022.2037273

[41] Hsu & Teng, "Activated Carbon Adsorption of Volatile Organic Compounds," 2000.